

Evolutionary theory of convective organization

Brian E. Mapes^a

^a *Department of Atmospheric Sciences, Rosenstiel School, University of Miami, Miami, FL*

Corresponding author: Brian Mapes, bmapes@miami.edu

Draft for submission, April 2, 2024

This Work has been submitted to Journal of the Atmospheric Sciences. Copyright in this Work may be transferred without further notice.

ABSTRACT

Observed patterns of convective cloud would be extremely improbable from random walks in an abstract space of configurations. Forcing is sometimes the driver, but complexity can also develop spontaneously. Here pattern evolution is considered as a natural selection process in a strategic game among configurations, akin to ecological succession. Information (-entropy) quantifies improbability, interpreted as Darwinian “fitness” to the extent larger-scale forcings are properly accounted. Reconciling inferred or revealed fitness with energetics could make convection a showcase of evolutionary theory, simply as reinterpretation of spectral kinetic energy (KE) budgets for dry convection. For moist convection, the flux [$w'E'$] of a total energy E , the teleological reason for convection, is conjectured to be the central resource of an evolutionary game, with water playing a constraining role like nutrients in ecology. Shannon’s information H is reviewed in context of evolutionary reasoning. Analysis of the ‘cloud botany’ shallow convection simulation set shows growth of H over tens of hours (perhaps more pertinently, with cumulative buoyancy flux). Anisotropy and precipitation boost H in qualitatively distinct and contingent ways, like separate species or ecological guilds. Deep convection over lowland South America also shows many-hour evolution times, beyond simple convective adjustment notions. If evolving horizontal patterns contain or imply information about vertical density profiles, they could become a new resource in data assimilation to predict larger scales.

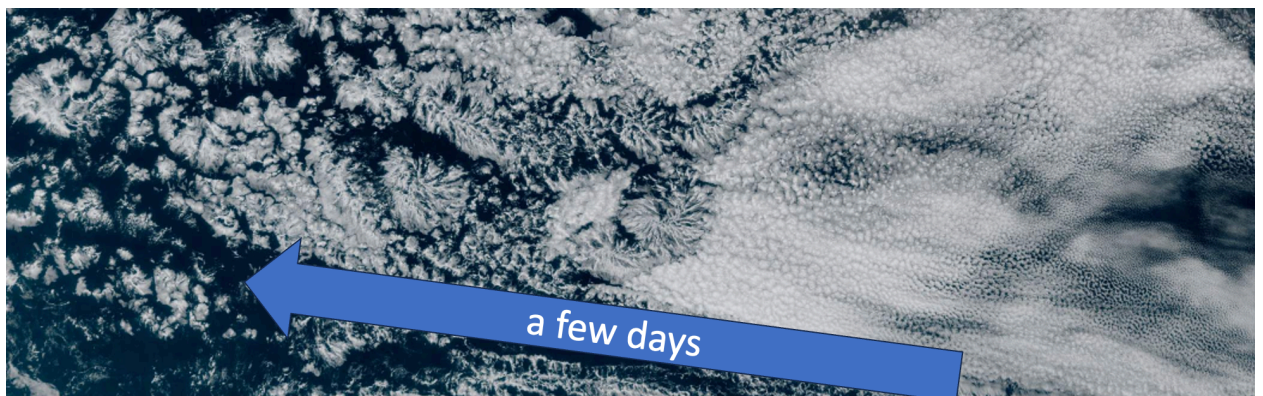
SIGNIFICANCE STATEMENT

Fine-grained cloud patterns are very complicated where vertical convection is happening. Might those patterns contain useful information about the convective process, for instance its efficiency and how that varies in space and time? Such information could be valuable to larger-scale weather modeling and prediction. To understand the nature of patterns, ideas from evolutionary eco-sciences (specifically, a succession process leading to unlikely cloud configurations) is interpreted as evidence of Darwinian selection or *fitness*. Quantifying this ‘unlikeliness’ of patterns, accounting for possible external sources, is the key analysis challenge. Techniques using information theory are brought to bear in two examples: a suite of shallow convection simulations, and satellite observations of deep convection development over tropical South America.

1. Introduction

Earth's troposphere is her most dynamic subsystem, short of life. Driven by interior cooling and surface heating, convection churns ceaselessly, in patterns loosely shaped by smooth latitudinal and wind-driven hydrography gradients and by sharper contrasts around continents. Time sifts these convective motions intimately, with gravity driving and friction damping certain facets or flow configuration more than others. A scientific account of tropospheric motions must therefore address this configuration selection filter, not merely the bulk energy source in the globally preferential descent of more-dense air.

Images of shallow and deep convective cloud fields are shown in Fig. 0, illustrating the evolution of complex flow structures from fairly uniform initial conditions. This essay views such development as an *ecological succession process*. Succession is different from a claim that actual airmasses (or ecosystems) have arrived in or even proceeded monotonically toward any well-defined equilibrium (or *climax*) state. Convective adjustment and other extremal principles (well-mixed layers, quasi-equilibria) represent such a climax assumption, and they suffice to some precision for some purposes. But the fine details of air density profiles are important to larger scales, and horizontal cloud patterns have direct impacts too, e.g. for cloudy radiation and precipitation statistics.



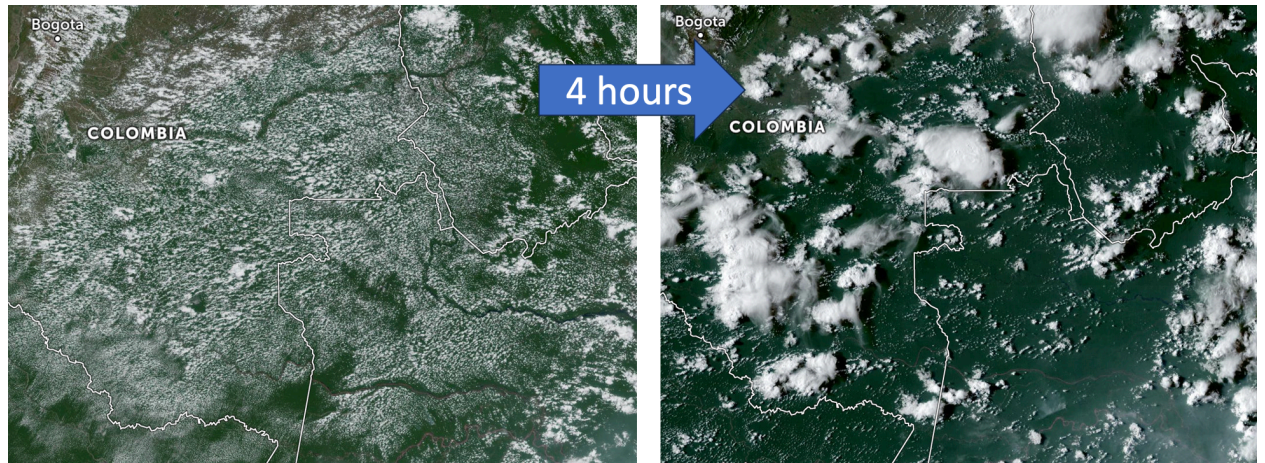


Figure 0: Top: Visible satellite image over the Southeast Pacific showing low-cloud configuration evolution through days of westward travel. Bottom: Evolution through a few hours in mid-day over the Amazon Basin. Images are from NASA Worldview, on days selected from just a few: the process is not rare.

No univariate measure can fully or uniquely characterize the abstract space of patterns or configurations. A cottage industry of devising morphometric indices of cloud-field “organization” has arisen, often driven by algorithmic convenience as much as by dynamical ideas. The reward -- modest bulk correlations with importance measures -- is motivating enough but is weak sauce. Intercorrelation matrices among morphometrics are quite complicated (Table 1 in Brune et al. 2021, codes in Janssens et al. 2021, Sakaeda and Torri 2021, supplement of Shamekh et al 2023). Here a Shannon information measure for configurations is advocated (Fig. 6 of Sullivan et al. 2019 is the only published example I found), rooted in (im)probability and thereby to an inequality-based scientific principle, evolutionary fitness.

Information as a framework for evolutionary reasoning is surveyed in Rosas et al. (2018), Golan and Harte (2022), Wong et al. (2023), and many cited references from complexity science. Assembly theory (Sharma et al. 2023) expresses a new information principle, perhaps too specific to molecular science. The *ascendency* principle, a kind of anti-Second Law inequality about information growth with time, culminates a “process ecology” (Ulanowicz 1997, 2009) viewpoint that provided important inspiration for this article. While convective cloud-field evolution lacks the ultra-long-lived extreme specificity of genetics, ecological evolution and economic game theory (Newton et al. 2016) share that limited-memory character, tallying relative populations of looser functional *guilds* that do the various jobs within an ecological network.

In the atmosphere, meso-scale patterns (*meso* meaning middle) are structures much larger than an *element* or *cell* scale (typically the depth of the convecting layer), yet far smaller than domain-controlled scales rooted in Earth’s geography. Mesoscales are mere affordances of Earth’s atmosphere: scales of motion which are free to develop but inessential. For example, mesoscale patterns lay beyond pre-satellite imaginings (Fleming 2007), a fruitful topic for discovery and description in the modern era (the memorable “gargoyles” in Zipser 1970). Now that the initial catalogue has been filled out, what is the research agenda? Machine learning (ML) offers new tools to get a handle on cloud patterns in imagery, but interpretation remains rather arbitrary, whether applied at instance level (“sugar-gravel-flowers-fish”; Rasp et al. 2020) or at category level after unsupervised category-contrast maximizations (Denby 2020, 2023). Might a theoretical frame help us to inspire, interpret, or orient ML characterization efforts?

One inference at stake in horizontal cloud pattern recognition is the associated larger-scale (scene-averaged) density profile (Stein et al. 2017), on which gravity then acts to drive larger scales. For example, the enforced scale separation in super-parameterization models (e.g. Pritchard et al. 2014, Tulich 2015) offers a clean laboratory to measure and interpret how different restrictions on mesoscale affordances (different-sized periodic explicit convection domains) rectify into performance issues of the larger-scale model. Evolutionary framing could lend scientific meaning to such domain-size experiments that have largely been viewed as mere computational engineering tests. If cloud pattern-to-profile retrievals prove robust, they could be valuable to data assimilation in regions with few vertical soundings, or shed new light on the shortcomings of parameterizations that ignore convection’s mesoscale evolution (Mapes and Neale 2011, Tsai and Mapes 2022).

To ready the ground for these possible new avenues for advance, section 2 offers a tutorial on elementary ideas of information theory, and some cautions around evolution’s tricky misconceptions (e.g. Gregory 2009). The information arithmetic of configuration spaces for 2D convective cloud fields is sketched out in section 3, illustrated with analysis of Cloud Botany simulations and observed South American deep convection in section 4. Section 5 summarizes and concludes.

2. Ideas from eco-sciences and statistical mechanics

Evolutionary logic since Darwin has been distorted by battling pre-scientific ideas for the ultimate story of life (e.g. Dennett 1996, 2017). Far below those soaring Natural History narratives, and related astro-biology debates about what to look for (Bartlett and Wong 2020), more mundane evolutionary reasoning enters the eco-sciences as mathematical frameworks. These include the specifics of spatial population ecology (e.g. Cantrell 2010), an abstracted “process ecology” elaborated by Ulanowicz (1997, 2009), and evolutionary game theory (Newton 2019) used mainly in economics.

In game theory, the unit of competition is not an individual agent or player, but rather a strategy, which can include collective or multi-agent patterns across time that need not even be explicit or conscious. Such strategies may best correspond to our convective configurations here, contending for energy gained through realizing vertical energy flux, while convective elements like “cells” are more like agents or players. Game theory’s stationary solutions (called Nash equilibria) need not be unique, nor even exist. Far more interesting are the myriad possible contingent pathways through networks of strategic (inter-)actors. The dynamics of ecosystems are almost always chaotic; for instance, Wikipedia at this writing states that “The balance of nature, as a theory, has been largely discredited by scientists working in ecology”. An evolutionary theory thus culminates not in a physics-style “solution” to a “problem”, but in a framework of explanation, made scientific by its conditional or logical predictions, which may be testable with experiments but often only in idealized ones. Such a theory is far less than a first-principles temporal prediction engine, or a recipe for successful technologies, but it might help to unlock improvements in those realms.

Closer to geophysical culture is the triumphal understanding of how statistical mechanics underpins thermodynamics, where continuum gas laws can be appreciated more deeply as statistical laws about molecular configurations. A primer on entropy and information will help some readers and is offered next.

a. Entropy as an information measure

In the computation age, weather model ensembles have helped inject probability concepts deeply and widely into atmospheric science (e.g. Palmer 2022). In the software age, information refineries now extract, blend, extrude and transmit information seamlessly among text, imagery, sound, and more, often based on the Universal Approximation Theorem. Exposure to these tools, and paying monthly bills for bytes, has given more and

more people a sense of *information*. It is helpful to relate and distinguish this from thermodynamic entropy.

In thermodynamics, entropy is the usual dual descriptor along with energy, but information is closely related (Parrondo et al. 2015). Many meteorologists have a vague sense that entropy measures something about ‘disorder’, culminating in the Second Law’s head-scratching principle that it tends to increase with time, expressing *undirected* evolution’s tendency toward most-probable configurations. For historical reasons, entropy was saddled with a source of confusion: units. In the words of *Farewell to Entropy* author Arieh Ben-Naim (2008),

Had the identification of temperature with the average velocity of atoms come earlier, it would have been more natural to define temperature in units of energy...[E]ntropy S would now be a dimensionless quantity...[instead of] the ratio of energy and temperature...The interpretation of entropy as a measure of [missing] information would have become much easier... This [interpretation] will not only remove much of the mystery of the unfamiliar word entropy, but will ease the acceptance of ... “the physical world as made of information, with energy and matter as incidentals.”

This dimensionless entropy $S = -\sum p \log(p) = \sum p \log(1/p)$ is a numerical measure of the nonuniformity of a probability distribution (PD) over some discrete domain like an enumerable set of configurations. It can be thought of as the expectation value of $-\log(p)$, with units of *bits or shannons* when log means base 2 (as used here), or *nats* (ln) or *hartleys* (\log_{10}). Since $\log(p)$ is a concave-downward function of p, S is maximum for a uniform PD, and is lesser for any nonuniform PD.

Entropy is best translated (returning to Ben-Naim 2008) as “*missing information*”. Missing from where? From any macroscopic-variables-only description that summarizes many elements, such as molecules in an atmosphere. Maximizing entropy defines *equilibrium*, a state where nothing is maintaining unlikely patterns against random interchanges or mixing. Entropy maximization expresses the propensity of closed systems to eventually wander into (and almost certainly never out of) the vastly largest volumes of their abstract configuration space, absent any guiding force to this wandering. This is the Second Law in probability terms: a claim which is tautological here because it is what we mean by “wander”, “guiding force”, and “eventually”. In the Bayesian (inferential) view of probability, maximum entropy translates as maximum ignorance or maximum uncertainty,

which is a humble prior place to begin inquiries, although an anticlimactic place for one's posterior to end up.

Simple, constant "guiding forces" (embodying constraints like conservation of energy) can easily be accommodated. Two familiar examples of maximum entropy PDs are informative, for an isothermal ($T = \text{constant}$) ideal noble gas atmosphere. 1. The *exponential is the maximum-entropy distribution for a given mean*. Given a potential energy ($gH = RT$), the familiar exponential decay of density with altitude in equilibrium embodies the maximum entropy principle. 2. The *Gaussian or Normal distribution has the maximum entropy for a given variance*. This is the Maxwell-Boltzmann equilibrium distribution of molecular speed, given the kinetic energy ($C_v T$ for a noble gas).

Information H is defined by comparing the entropy of any PD with a uniform PD over the same discrete domain.

$$H = \text{"information entropy"} = \text{maximum entropy} - \text{actual entropy}$$

The utility of this quantity hinges on how strategically one defines the domain of the PD-- in this case, how we define and count "elements" of a convecting flow and their set of possible "configurations". If the base 2 logarithm is used (as here), the naïve improbability of any given macroscopic configuration defined by its PD is 2^{-HN} with N a measure of sample size. Showing the existence of non-randomness (less-than-maximum entropy) is dull, a mere statistical detection problem. A deeper evolutionary theory of how the improbable arises by selection can be aided by quantifying *unforced increases of improbability with time*.

b. How convection is unlike biology

Biology is rooted in chemistry, subject to the laws of molecular thermodynamics. Physico-chemical scientists have long grappled with life as a problem in the non-equilibrium thermodynamics of open systems (e.g. Schrodinger 1944, Nicolis and Prigogine 1977). Life's vital variety is *permitted* because Earth has energy flowing in and out, but that is different from explaining it. The lower entropy of fewer hotter photons in sunlight, compared to Earth's emitted radiation, *allows* chemically based life to build complex (unlikely, low entropy) macroscopic structures, at the cost of a tiny bit of extra entropy production. Attempts to turn this entropic allowance or affordance into something more incisive have not been very fruitful, beyond helping to close off naïve second-law objections to the very possibility of life's existence. Physico-chemical entropy constrains the evolutionary liberty of

life only a meaninglessly tiny bit, mainly at chemical frontiers of physiology and metabolism shared by all kinds of cells. The bewildering web of life on Earth teaches us that evolution is not a winner-take-all optimization process, but rather a highly nonunique (history dependent) causal network process operating on long timescales, mediating among tighter causal loops inside multicellular bodies, which mediate among the even more intimate contests among chemical causal loops inside cells.

In geophysical fluid dynamics, attempts have been made to translate principles like *maximum entropy production rate (MEP)*, from weakly non-equilibrium thermodynamics theory, into constraints on macroscopic flows (see review in Singh and O'Neill 2022). Again, these efforts seem unincisive. To quote those authors: “The MEP principle is understandably appealing ... Yet the principle lacks theoretical justification as well as consistent numerical and observational success. We conclude that the validity and usefulness of the MEP principle remain aspirational.” In the currency of thermodynamic entropy, the excess produced by macroscopic phenomena is less than a drop in an ocean. Gray dust on the moon has no trouble converting sunlight to lukewarm thermal radiation without life or circulating fluids. The thermodynamic entropy budget of the atmosphere has been computed, but is predominated by terms near the chemical frontier, like mechanical viscosity in raindrop wakes and diffusion down hyperlocal humidity gradients around droplets (Pauluis and Held 2002, Romps 2008). Usefully binding or incisive constraints on macroscopic flow configurations are not obvious.

Carnot's heat-engine efficiency and the “free energy” concepts of Gibbs and Helmholtz set an upper limit on the mechanical energy of macroscopic atmospheric motions (the rate of work that be extracted from a gas, given its continuum equation of state). This constraint is based on the temperatures *of air* at the locations where heating and cooling occur, not the quality of the photons doing the heating and cooling. Since the circulations in question help shape the temperature field itself, this is not a truly external constraint. Still, basic troposphere-stratosphere lapse rates are robust enough to the details of tropospheric convection that Carnot's limit sets an upper bound on, for instance, the most intense hurricanes possible in a given climate (Emanuel 1991). Flywheel-like rotational motions protected from surface friction can accumulate large amounts of KE, even though the source rate is limited this way. This KE may itself become another energy resource for the competitive games of convective configuration, if kinetic energy extraction via momentum

transport becomes comparable to buoyant production. Here we will limit our focus to thermal convection, drawing only on potential energy production and storage and conversion to KE via the covariance of vertical velocity w and buoyancy b , $[w'b']$.

Table 1 summarizes important differences in the evolutionary reasoning applicable to biology vs. convection. Columns distinguish life's hyper-specific and verbatim-reproduced genes (left), multi-agent ecological or economic games (middle), and convective flow configurations to be examined here (right). The time scales (first row) on which 'fitness' is adjudicated depend on the memory or lifetime of contending strategies. For selfish genes (Dawkins 1976) this is geological, millions of years. For ecosystems the longest memory in a fitness competition may be the lifespan of large animals or their cultural coalitions. For configurations of convecting flow, the inertia of divergent wind may hold their identity (a container in which fitness-achieved gains may accrue) for minutes to hours. Active tracers like water vapor and vorticity extend this memory to features with traceable identity for hours to days.

| Table 1 | Genetic evolution | Eco- & game theory | Conv. configurations |
|--------------------------------|--|--|---|
| Timescale of evolution | Geological, phylogeny (DNA) | Lifespan of agents, strategies, & niches created by others | Inertia of elements (hours), active tracers (days) |
| Fit means what? | Fitness of innovations determined within phenotype (cells, tissues, organs) | Depends on heterogeneous network, <i>i.e.</i> on other successful entities, guilds, & strategies | Fitness of <i>elements</i> & <i>configurations</i> is ours to define for convenience and meaning; we are interpreting budgets |
| Role of configs in energy flux | Teleology is a historical-religious delusion that must be forbidden in evo discourse | Strategies may have some purposeful intentions, especial in social sciences | Teleology is a correct guide to the fitness function: convection exists for a larger-scale demand for energy flux |

Table 1. Similarities and differences of evolutionary reasoning in different fields

What is fitness (the second row)? The answer is always contingent on an environment: an open system with energy flows that provide opportunity for individual

entities, and a context of other entities to interact (compete, cooperate) with. In the genetic realm (left column), innovations face trial in the intimate chemical context of the cell, then within the body, and only more loosely in an environment of other bodies and multi-organism social strategies (middle column). For convection, we cannot answer the question of fitness before defining what our *elements* and their possible *configurations* are (section 3 below). These definitions are nonunique, but must be a sensible basis set for contending *strategies*: entities or containers with a lifetime and identity long enough, and sufficiently well defined, to accumulate the gains and losses that define an evolutionary game.

Crucially (third row in Table 1), the question of telos (“purpose”; Aristotle’s “final causes”) must be confronted. Darwin and his intellectual heirs have faced centennial struggles to differentiate science from comforting faiths about the ‘purpose’ of life. Invoking purpose (orthogenesis or vitalism) can short-circuit evolutionary lines of reasoning at any point where sophistry cares to deploy the tactic. Biology has evolved (not a pun!) an intense vigilance against this discourse tactic. As mentioned above, life is *permitted* by the Earth’s energy and photonic-entropy budgets, but macroscopic forms are not meaningfully constrained by those. In stark contrast, convection is *structural* to the Earth’s energy budget, and not at all dependent on the photonic entropy of the incoming radiation. That is, the *purpose* of convective flows is almost identical with their energy transport efficiency – but only almost.

For dry convection, the *thermal buoyancy* acceleration b gives immediate, local KE feedback to successful (rising and buoyant) flow elements, quickly redistributed by pressure in its role as mass continuity enforcer. For moist convection, where b is not directly related to total thermodynamic energy (for instance, the virtual effect of vapor on b is only about 1/6 that of its impact via latent heat release when condensed), might a looser form of efficiency-reward still enforce the teleological “purpose” of convection more indirectly? For instance, a drying of the unsaturated environment by organized cloud systems actively suppresses random-cumulonimbus competitors (Tsai 2023, Tsai and Mapes 2024). Can this competitive strategy be adequately tallied in a total-energy budget?

With this preamble of terms and ideas established, we are ready to sketch an evolutionary framing and logic for cloudy convection’s mesoscale non-uniformity. With fitness measures, mesoscale structure might be escalated to “organization”, seeking to relate form to its function in the overarching terms of Mapes (2021).

3. Elements, configurations, and competition

As alluded above, right-sizing a countable configuration space is essential to an accounting system for evolutionary effects: The absurdly numerous ways that 10^{25} molecules can be arranged has nothing to say about the (im)probability of multi-cell storms given a convecting sky. In his book *The Big Picture* (2016), elaborating on Aaronson et al. (2014, said to have an update in the works), natural philosopher Sean Carroll calls the information of macro-scale configurations *complexity*, distinct from the vastly greater micro-scale or thermodynamic entropy obeying its Second Law. His example is hot coffee over cold milk (simple), becoming a turbulent swirl after stirring (complex), and then a final mixed state (simple again) even as *thermodynamic* entropy increases monotonically.

Here we wish to define convective flow *configurations*, composed of flow *elements*, which in a similar manner can evolve or decay in *complexity*. We want to estimate how *improbable* a complex configuration is, relative to the statistics of an unguided long wander in configuration space. That improbability has a self-organizing component indicative of evolutionary *fitness*, which we want to isolate from a part inherited from large-scale forcings and boundary conditions. Total success would be to reconcile this ‘fitness’ inferred from the growth of configuration improbability with more mechanistic measures of fitness rooted in energy budgets, direct measures of strategies and payoffs in the temporal game theory of a competition for the limited driving resource of vertical energy flux (destabilization).

Three obvious choices for “elements” of complex convecting flows might be:

1. Pixels in a convection-resolving mesh, labeled as “cells” or not.
2. Finite-sized cloud *objects*, meters to km and beyond, far above molecular effects.
3. Fourier *wavenumbers* (truncated to a minimum wavelength of many meters).

If the logic of evolutionary explanation is true, the information budgets of these different configuration basis sets should be reconcilable. Such an exercise could usefully illuminate the connections between well resolved Eulerian mesh budgets, turbulence spectra in Fourier space, and coherent structures. That goal may be a generational timescale aspiration.

a. Illustration: pattern entropy of clouds on a grid

Many of our target phenomena are tallied as connected-pixel *objects* in condensed-water fields from satellite, RADAR, or models. For deep convection, such observationally convenient boundaries define Mesoscale Convective Systems (MCSs, Houze 2018, Chen et

al. 2022) for instance. Here the moniker of “systems” is more a marker of the existence of internal heterogeneity, rather than any claim of a *closed* system whose fate is in its own hands. But even a cumulonimbus cell is a compound entity, with updrafts conceptualized as multiple “bubbles” or “thermal chains” (Morrison et al. 2020), and downdrafts important, and on and on to puffs and gusts. In short, it must be for strategic reasons that we choose how to discretize and enumerate the “elements” of convection, as our science lacks a fundamental basis of atoms (Greek for un-cuttable) or cells (meaning walled enclosures) or individuals (again, un-dividable) enjoyed by chemistry, biology, and social sciences.

For simple definiteness, consider “configurations” as applying spatially at an instant, in the form of discretized locations (x,y) of N cloud objects of undistinguished properties in a square horizontal domain (or map) indexed with $2^r \times 2^r$ boxes. Here r is the logarithmic *resolution* of our location accounting (depicted as $r=4$ by the $16 \times 16 = 256$ boxes in the mesh). Maximizing resolution for r is not an ideal; a scientific strategic choice should be made rather than always defaulting to the exigencies of data sources.

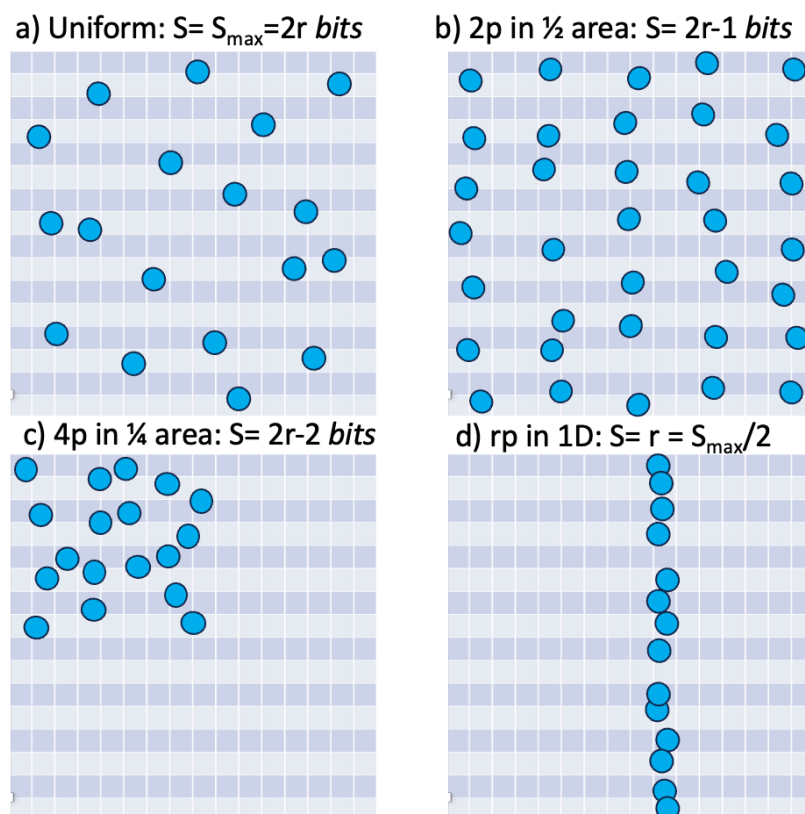


Figure 1: Probabilistic configurations of clouds on a map, and their Shannon entropy S per cell.

Some example configurations are shown in Fig. 1, with the underlying PD and its entropy named in each plot title. The maximum-entropy configuration (panel a) has the most

“missing information” of any description: cloud probability $p_{\text{cloud}}(x,y) = p_{\text{uni}} = (r^2)^{-1}$ is uniform over the domain. Summing up the formula $S = -\sum(p \log p)$, or simply noting that the expectation value of $-\log p$ is its value anywhere in this case, the result is $S_{\text{max}} = 2r \text{ bits}$ for each cloud. Compare that to the case where clouds are randomly distributed in only half the area, for instance within the crests of a square wave in x (Fig. 1b). With zero weight in the empty half (since $p=0$), the expectation of $-\log p$ is its value anywhere it is nonzero: $-\log(2p_{\text{uni}}) = -\log(2(r^2)^{-1}) = S_{\text{max}} - \log(2)$. Using the base-2 log this is $S_{\text{max}} - 1 \text{ bit}$.

Try the “missing information” understanding of entropy to think through the case where the clouds are uniformly probable within only a specific quadrant of the domain (Fig. 1c). Compared to the random case, two *bits* of information are now known for each cloud’s location: which half of the map horizontally, and which half vertically. Subtracting from S_{max} , we obtain $S_{\text{quad}} = 2r - 2 \text{ bits}$. Notice that the same result can be recovered by the forward construction used above: $p = 4p_{\text{uni}} = 2^2 p_{\text{uni}} = 2^2 (2^{-r})^2$ and the Shannon entropy formula indeed confirms $(2r-2) \text{ bits}$. A stronger entropy change is implied by dimension reduction: if p is uniform only within one line on the map (panel d), p is (2^{-r}) rather than $(2^{-r})^2$, so S_{line} is $\frac{1}{2}$ of S_{max} .

The above calculations assumed we know the *actual underlying PD* of each case. From observations of specific scenes, this probability must be estimated somehow. This is a nontrivial exercise and indeed, a high craft of natural philosophy. Frequentist composite building can be done straightforwardly on a set or pool of instances, at a given discretization resolution. But choosing which instances are philosophically interchangeable and suitable for pooling, and choosing a clear and accurate moniker for that pool, is the heart of the problem. The finer the bins (to resolve distinctions), the more often-heterogeneous data must be pooled to fill them (blurring those fine distinctions). At full resolution, any highly detailed scene is extremely improbable, like a QR code -- whether it resembles a company logo or a spilled domino truck. Seeing a pattern in a single cloud photograph is not science.

It is straightforward to extend configuration descriptions to account for additional distinctions: a space x time mesh, discrete categories for sizes or depths, or any other countable categorical properties. Although probability is unitless and confined to $[0,1]$, to be built up from data by averaging sparse Boolean arrays of 0 and 1 values, the clean categorical structure of PD-based analysis helps to spotlight the analyst’s strategic scientific distinctions. Significance testing is structural, it comes along for free; indeed, p-value is improbability.

How *improbable* is the configuration in Fig. 1c, with $N=20$ cloud objects in the upper-left quadrant of the domain? Does its existence demand -- or in other words, stand as evidence for -- a special causal explanation, whether that be a patterned forcing or an evolutionary process operating in the past? This is null hypothesis testing: might this scene have arisen by chance from an underlying uniform distribution? The answer is easy here. The probability of each cloud object appearing in the upper-left quadrant is $\frac{1}{4}$, and 20 clouds have done so. The chance of coincidence (that is, the improbability of the configuration, *relative to uniform*) is $(\frac{1}{4})^N = 2^{-(N+H)}$ or 1 in 2 million for 20 clouds and $H=2$ bits. This could become 1 in 1 million, $(\frac{1}{4})^{19}$, if we reframe the question to “how improbable is it that 20 clouds ALL appear in ANY ONE quarter of the domain by uniform chance?” Then only $N-1$ clouds must be explained to have joined the first one in whatever quadrant it arose in. Estimating the (im)probability of a nonuniform PD may be a bit subtler for an arbitrarily large number of samples in a histogram, whose information difference from uniform PF (called Kullback-Leibler or K-L divergence) converges to a stable value, often a small fraction of a bit (section 4 below).

The summary for later use is: spatial clumping *subtracts* information from S_{\max} according to the log of the enhancement of probability in confined areas; dimension reduction to a *line* halves the entropy S_{\max} of a 2D uniform distribution; and zero entropy is implied by a fully determined configuration (no missing information), such as one cloud per hilltop on a given topographic lower boundary condition (BC) field.

b. Spectral ‘elements’ in dry convection

Convection’s flow configurations need not be cloud locations on spatial maps. For the simplest atmosphere-relevant case of dry convection (no phase change, no stratification at equilibrium), with a buoyancy source at the bottom and buoyancy sink throughout a cyclic or infinite fluid layer, Fourier decomposition would be a natural choice. The orthogonality of wavenumbers makes the spectral kinetic energy (KE) budget complete and tidy, by Parseval’s Theorem. Evolutionary competition for the limited KE source $w'b'$ (in this case a true “flux” of conserved b) is simply a theoretical re-interpretation of that budget. Feedbacks between a configuration’s KE and the portion of its induced source $w'b'$ that projects back onto that configuration can be computed. Might the slopes of equilibrium or “saturated” spectra be interestingly reinterpretable in these ecological terms? Even if so, orthogonal harmonics are merely a basis set.

Suppose the ‘fittest’ convective flow configuration is a long surface fetch picking up buoyancy, feeding it into an updraft that is wide enough to be not too diluted nor resisted by diffusion, but not so broad that the radiative cooling-like buoyancy sink has much time to act during its ascent time through the layer. The Fourier description involves many wavenumbers conspiring in a group strategy, cohering in both amplitude and phase. The development of this strategy would probably take many turnover times of the naïve, easily-formed cells of aspect ratio near 1 which initially form from uncorrelated noise after switch-on destabilization (e.g. Vieweg et al. 2021). Its probability of developing without the steering effect of a fitness advantage might be vanishingly small, so finding such a configuration might allow strong inferences about that fitness-driven evolution process. Quantitative descriptions (e.g. Vieweg 2023) may not exhaust the possible insights to be gained.

Fourier phase spectra are cryptic, a tricky informatic puzzle, so diagnosing such a multi-wavenumber strategy in spectral budgets would not be straightforward. Perhaps machine learning could discover such wavenumber coalitions, or wavelet methods (Rajković et al. 2017, Brune et al. 2021) might help. Learning to monitor evolving flows for such emerging winner or survivor configurations, and to reconcile results with energy-budget rigor, seems a fascinating and ready challenge. Preliminary attempts at an example remain incomplete and too complicated for the present scope.

c. An information space of interactions: the Lotka-Volterra equation

Whatever our discrete space of configurations, orthogonal or not, indexed by whatever measure with a letter i or j , interactions can be accounted for. A famous continuous prognostic equation for future number n_i of configurations of type i may be written with an interaction matrix in the [generalized Lotka-Volterra equation](#) (see Wikipedia):

$$d/dt(n_i) = F_i n_i + \sum_{j=1}^N K_{ij} n_i n_j$$

External forcing or ‘food’ F_i is formally partitioned by configuration category i , although in our case it is perhaps more like a constant: widespread destabilization of the fluid layer. Interactions within the matrix \mathbf{K} can include negative competition ($K_{ij} < 0$), positive mutualism ($K_{ij} > 0$), and “predator-prey” or transformation terms ($K_{ij} K_{ji} \leq 0$, driving configurations across category boundaries).

An example of Lotka-Volterra discourse for convection is Nober and Graf (2005), using the traditional “cloud types” (plume top heights) of Arakawa and Schubert (1974, AS74). Going beyond AS74’s assumption that plumes are independent except via their common uniform environment, a fuller interaction matrix \mathbf{K} can be considered. Yano and Plant (2016) elaborated this theory much further, to the point that a reader must hope their vast Eq. 9, with countless terms if expanded out, was made safely by algebraic symbol-manipulation software! Matrices like \mathbf{K} could be a useful mathematical currency of our desired evolutionary theory, although we need not confine interactions to linear matrix multiplication nor write the continuous calculus limit of $\Delta t \rightarrow 0$.

As a sketch space, this \mathbf{K} matrix view over one “time step” is illustrative of some useful ideas. For the sake of argument let us index configurations by their mesoscale cloud pattern entropy S using the ideas of section 3a. Randomly scattered cells are the maximum entropy configuration, at the high ends of the x and y axes. Lines with half the maximum entropy are the low ends. Waves and blobs (subtractions from S_{\max} as narrated in section 3a) lie in between. The all-negative competition for a limited energy resource is suggested with orange-red shading in Fig. 3. All kinds or configurations of convection at time t (the x -axis) have a negative (orange-red) impact on all kinds at time $t+1$ (y axis). But this competitive influence is nonuniform.

A simulation result supports the tilt of the shading in Fig. 3: In a uniformly destabilized cloud model, Tsai (2023) showed that a shear-induced belt of squall line-like storm configurations drives the domain mean atmospheric profile toward a more stable and drier profile than random convection produces, or can thrive in. In this way, line-like storms suppress the growth of random cells, “winning” the competition for moisture (rainfall) and presumably for energy flux and KE budgets (not computed there). These squalls were thought to be buoyancy-driven, not tapping shear KE importantly, but selected by gravity according to their hardness to shear, and/or actively boosted by shear-cold pool interactions. Once they develop after shear switch-on, in a complex succession process involving destruction of their competitors, the bulk density and moisture profiles are indeed affected, as would be felt by larger scale flows if not forbidden by cyclic lateral conditions.

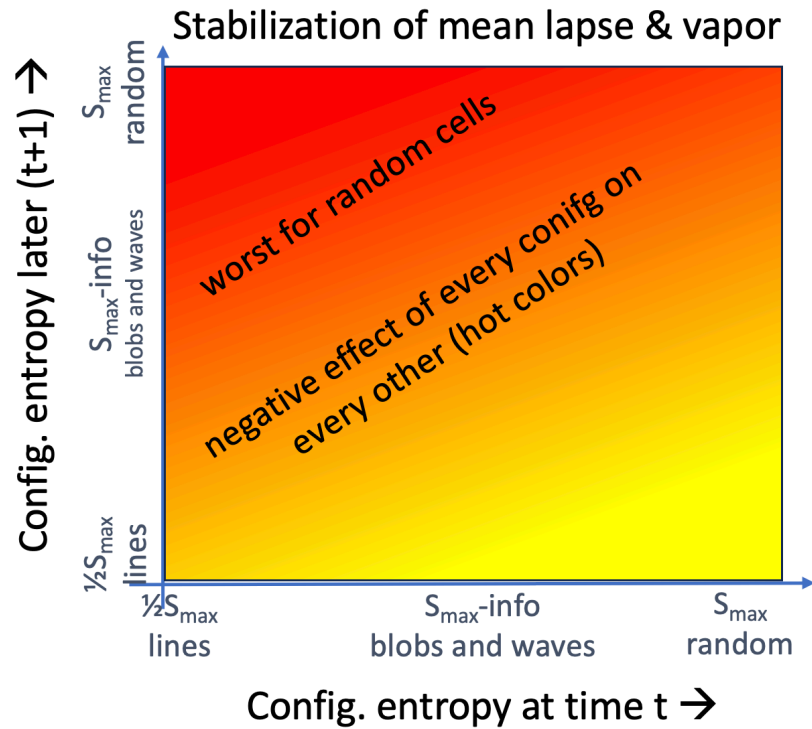


Figure 3: A negative interaction: the stabilizing effect of convection, expressed as bad (orange-red) contributions to future (y axis) convective elements (configurations) from various elements in the present (x axis). Both axes are indexed by the spatial entropy (negative of information H) as in Fig. 1.

Quantifying more such interactions in $S_t \times S_{t+1}$ space could be the currency of an evolutionary theory. The many facets or components of configuration “fitness” may be highly situational, particular to categories (waves vs. blobs), contingent (expressing nonlinearity), etc. To illustrate a few other such “fitness” ingredients, Figure 4 speculates about some positive (depicted as blue-to-purple) partial effects or factors that may drive configuration evolution.

Figure 4a indicates ease of formation of new cells at $t+1$. This favors high- S configurations (random cells) by definition, proportional to the sheer numerosity of such configurations. In panel b, a related decay process of low-entropy structures like lines or blobs at time t is depicted as an up-entropy wander (shading is above the diagonal). Panel c indicates cell-neighbor-favoring processes, for instance from cold-pool triggering effects (Zuidema et al. 2012, Haerter 2019, parameterized for instance in Frietas et al. 2024) or ‘preconditioning’ of moisture (Randall and Huffman 1980, Hohenegger and Stevens 2013). These effects are suggested to make clumps grow, decreasing configuration entropy (shading is depicted below diagonal). Panel d considers the role of larger-scale isotropy-breaking processes such as vertical shear or horizontal deformation. Blue (positive) influences near the

bottom drive configurations toward lower values of S (whether the $S_{\max}-2$ of cloud streets or the $S_{\max}/2$ of a narrow frontal line). Here shading extending far over toward the lower-right corner to suggest that even nearly-uniform random configurations at time t might quickly and directly be driven toward very low-entropy lines at time $t+1$ by deformation, for instance.

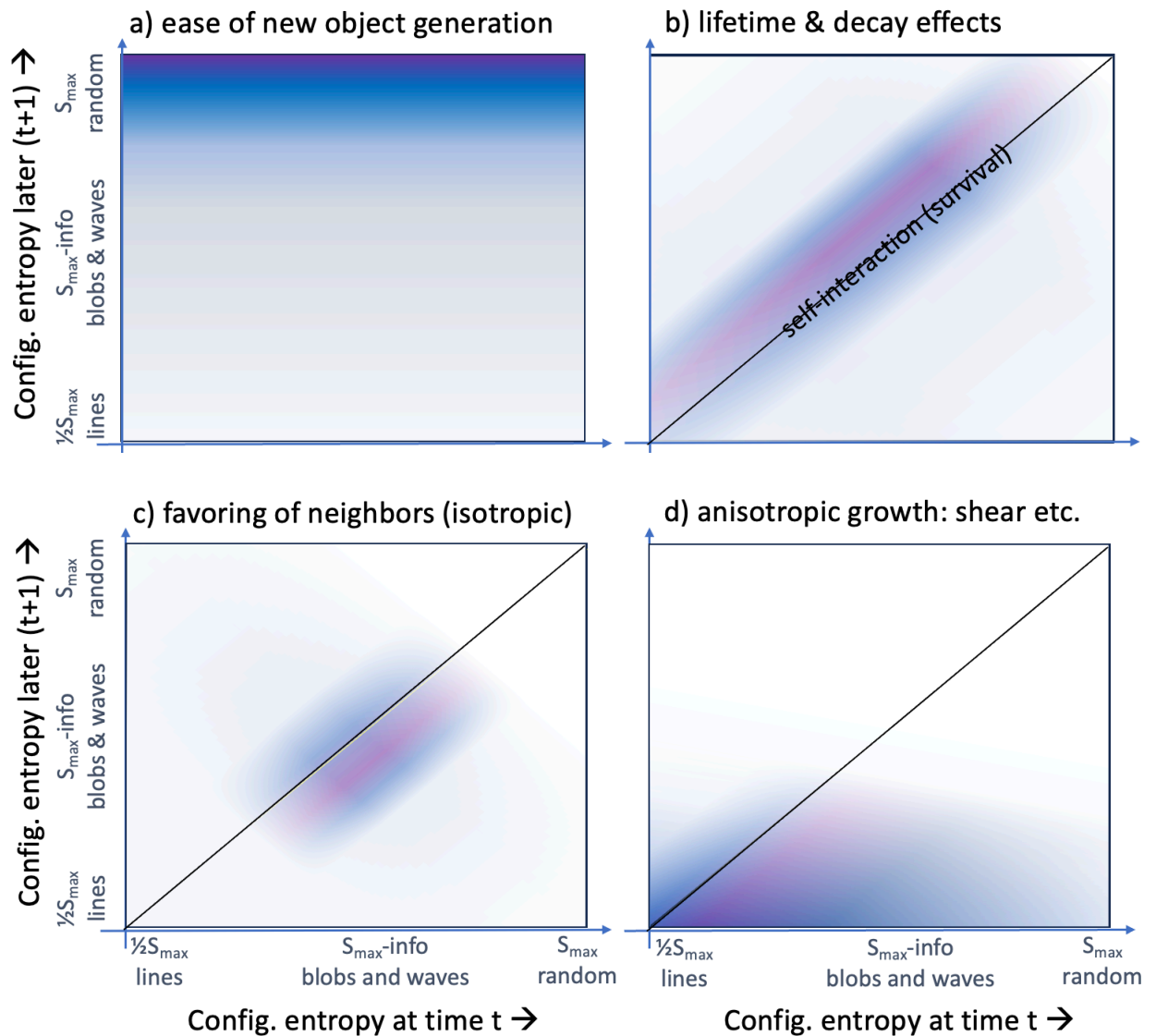


Figure 4: As in Fig. 3, but for selected positive effects (indicated by blue-purple shading). a) The sheer numerosity 2^S of available configurations favors random cells and configurations easily reachable by a random walk from there. b) Random erosion of persisting lower- S configurations is indicated as positive shading above the diagonal. c) Nearest-neighbor favoritism lowers configuration entropy (shading depicted below the diagonal). d) Large-scale wind shear or deformation drives dimension-reduction toward linear structure (shading is concentrated at bottom).

Many kinds of simulations and data diagnoses could contribute components to such a $t \rightarrow t+\Delta t$ configuration space of interactions, and justify its generalizations or extensions. The goal of this essay is to inspire such efforts, not bound them. To be a bit more specific, the next section shows data analyses of shallow and deep convective cloud fields utilizing configuration entropy, in hopes of firming up the path forward.

4. More rigorous preliminary analyses

Succession after disturbance is a very informative situation for ecological understanding. Easy entities emerge first while more-efficient but more complex structures take time to develop along adjacent-possible pathways. Simulations with clean initial conditions and uniform lower boundary conditions are the convection equivalent, and section a considers this case for shallow convection over subtropical oceans. Section b tackles the harder case of observational data, using fairly-uniform geographical comparisons (lowland South America and the South Pacific) to quench climatological structure and reveal evolution in time.

a. Shallow convection configuration evolution in the cloud botany simulations

Shallow cloud patterns are amazingly diverse. High-resolution simulations suggest that 160km may be the largest scale of spontaneous evolutionary organization, and about 30h its time scale (Lamaakel et al. 2023). With more effort, simulations could offer an opportunity to reconcile cloud-object configuration descriptions with spectral flow-configuration accounting (as suggested in section 3b), beyond the current scope of effort. Supervised (Rasp et al. 2020) and unsupervised (Denby 2020, 2023) machine learning are beginning to get a handle on patterns. One predictor of complexity might be *evolutionary depth*, perhaps monotonic if not exactly proportional with convecting air mass *age* (time since last stabilization), as suggested in section 5.2 of Schulz et al. (2021). Might a neural network learn to predict an *age* label from spatial cloud-scene patterns alone?

But is simple elapsed time the best measure of the convection's level of evolutionary development? Perhaps a vigor-weighted measure is needed, like a rescaling of time in eddy turnovers, or (here, for simplicity) *kinetic energy throughput*: the indefinite time integral of domain mean $[w'b']$ from a cold start. The new Cloud Botany simulation ensemble (Jansson et al. 2023) presents a great opportunity to explore these questions through analysis of an open Web-hosted dataset (details are in this article's supplemental code notebooks).

Each of Cloud Botany’s 103 simulations began from a uniform initial state over a uniform water surface, so all pattern development is spontaneous, conditional only on patterns at prior times. Figure 5 shows snapshots from simulation 97 of at times 5, 24, and 53 hours into its duration. These simulations span 2 diurnal cycles of interactive radiation and complex inertial oscillations from initially geostrophic flow at a subtropical latitude. Initial clouds are spotty (left panel), but after a day streets of concentrated cumulus activity are evident (middle). After 2 days, precipitation develops and its dynamics (re-evaporation; downdrafts; spreading cold pools; triggering by pool-edge gust fronts) soon dominate the spatial configuration (right panel).

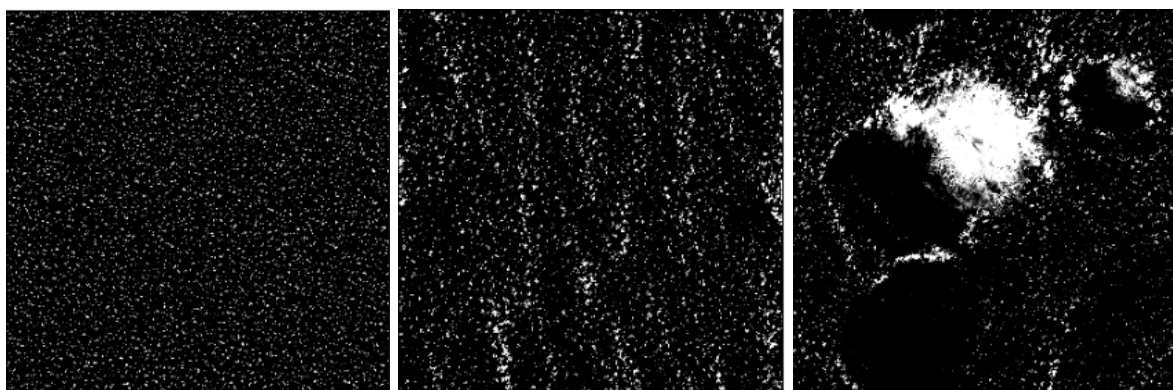


Fig. 5: Cloud fields from ensemble member 97 from Jansson et al. (2023) at times 5, 24, and 53 hours into the configuration succession process. Domain size is 153km. Qualitatively different dynamics begin after precipitation develops (right), a process whose timing depends on anisotropy (center), aided presumably by the ENE surface wind with westerly shear.

As a measure of mesoscale information, $H = -\sum(p \log p)$ was computed at periodically subsampled times in each simulation from a 32x32 bin (4.8km bin size) PD of cloud water path being above its upper spatial decile. To estimate this PD, Boolean arrays of 256x256 pixels (down-sampled from the original 1536x1536 100m cells to reduce data volume), with ones covering 10% of the area, were averaged into 32x32 boxes uniformly covering the 150km domain. Scenes with <10% cloud cover were discarded as the decile is undefined.

Scatter plots of this H are shown in Fig. 6, vs. simulation time (left) and vs. time-accumulated [w’b’] (right). Colors lighter than purple indicate significant time-accumulated precipitation. Green-yellow dots show that precipitation can quickly produce a qualitative boost in H, akin perhaps to a new *trophic level* (predators), or more agnostically a *guild* (a functional grouping of organisms in an ecosystem), and can achieve higher values of H than the nonprecipitating cases (purple dots) ever do.

Setting precipitation aside for a moment, Fig. 6a indicates that H increases for many hours from the uniform starting conditions, but it also can decrease when radiation stabilizes the convective process (hours 30-40 in left panel). A naïve bulk estimate of decay time for w variance, $[w'w']/[w'b']$, is less than a half-hour, but horizontal branches of mesoscale flow patterns can store KE for 10s of hours, agreeing with the 30h result in Lamaakel et al. (2023).

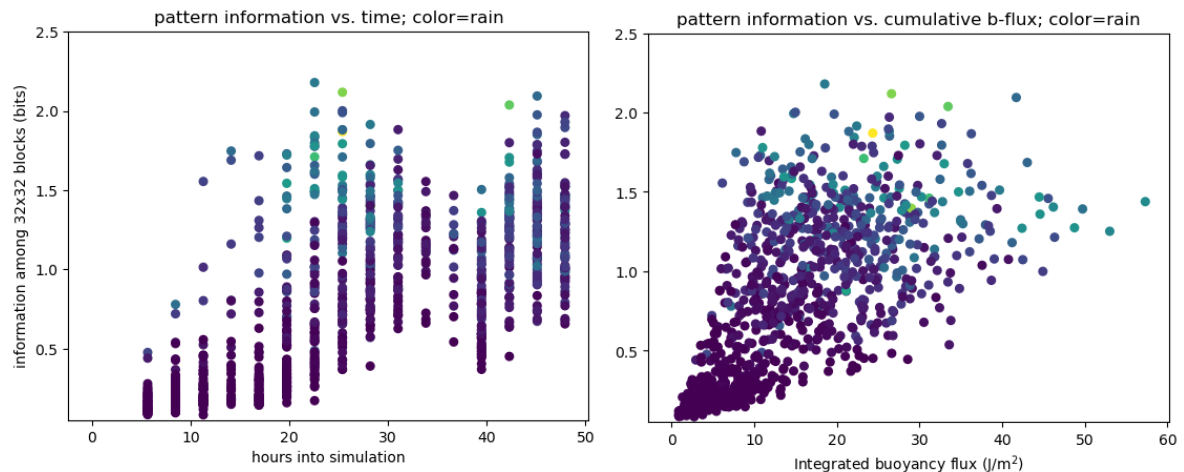


Fig. 6: Scatter plots of mesoscale (4.8 – 150km) cloud water pattern information H (a measure of deviations from spatial uniformity) vs. time (left) and KE throughput (time-accumulated buoyancy flux, right). The color of each dot expresses time-accumulated precipitation, with purple reflecting nonprecipitating scenes.

KE throughput or integrated buoyancy flux (right panel of Fig. 6) seems to pretty well predict a lower bound of H , although the range of H values for IBF of 10 - 20 J m^{-2} is quite wide even in nonprecipitating cases (purple). Linear structures like the middle panel of Fig. 5, whether indicative of resonances with waves or momentum-instability roll circulations, are often involved (based on image perusal). These may also deserve to be treated as another separate ecological guild (or two), offering a shortcut to mid-range values of H and possibly to precipitation. Quantifying these interactions between configuration categories is beyond the present scope, but straightforward: the web-hosted Cloud Botany dataset contains enough information and this paper's supplemental repository provides strong code starting points.

b. Precipitating deep convection configuration

Precipitation is such a powerful pattern-making process that this section spotlights it, by analyzing deep convective cloud fields. Again the temporal process of succession is observed after a stabilizing event that wipes out the convection (night-time over land). The climax

ecology of convection over warm ocean, where the fitness selection game never ceases or re-initializes, is used as hypothesized asymptotic limit of this succession process.

As input data, 3-hourly IR imagery data during daytime (at the same five time levels each day with 0.07° resolution (hereafter approximated as 8km), covering 20x20° lat-lon boxes over South America (SA, 20S-0S, 46W-60W) and the South Pacific (SP, 20S-0S, 145W-165W), were obtained from the NOAA Gridsat dataset (Knapp et al. 2011). Our samples include 235 days in SA (145 days in SP), spread over 20 years. These are the days on which a Mesoscale Convective System (MCS, as defined by Chen et al. 2023) was identified to initiate in somewhat larger spatial boxes at a specific local evening hour (23UTC in SA, 9UTC in SP), but that criterion is not important except as a general wet-season selection, as revealed by comparisons with another 235 days exactly 1 year later. That reference set has identical diurnal and seasonal sampling, but different weather and no specific selection criteria on the day, yet its statistics are very similar (not shown here; see code notebooks in supplemental repository).

Defining convective “cell” entities on this approximately 8km pixel mesh lets us tally information about their possibly-nonuniform probability patterns, as in Fig. 1. To define cells, IR temperature is very lightly smoothed (with the *scipy* library’s *gaussian_filter* function using $\sigma=1$ pixel), and then local minima are identified with that library’s *minimum_filter* function. Minima whose T is colder than -40C are declared to be deep convective cells. These choices satisfy the eye (Fig. y) and were made on that basis (illustrated in Fig. 7).

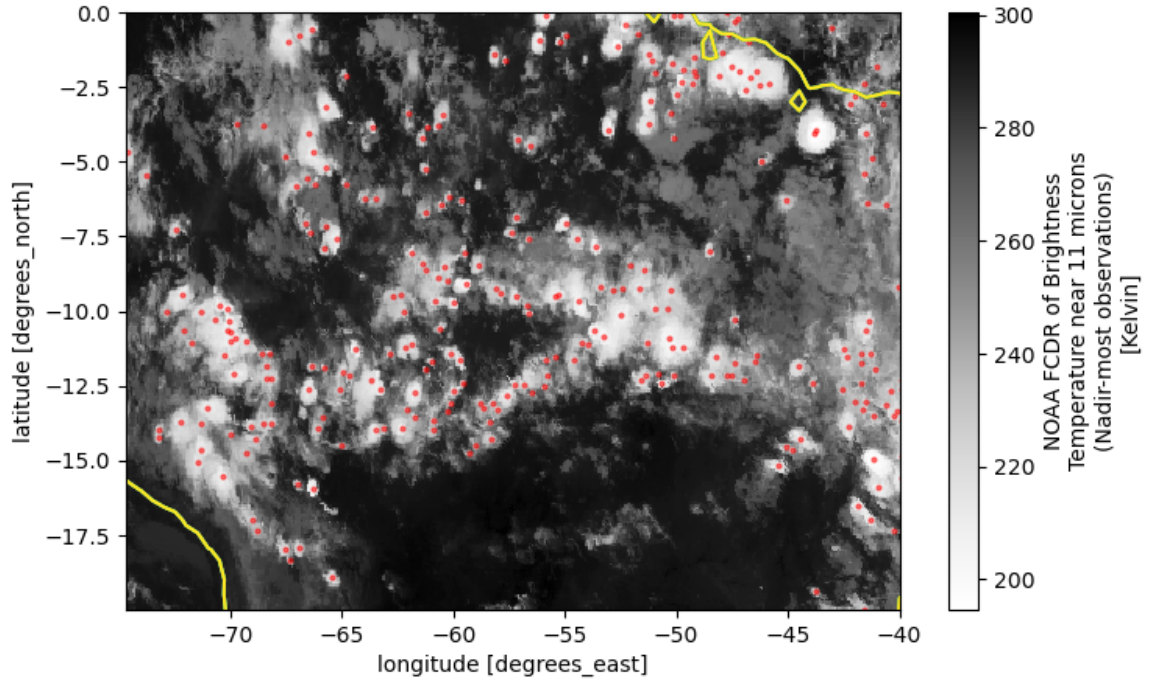


Fig. 7: Cell identifications (red dots) as local minima in lightly smoothed IR imagery with $T < -40C$.

Summing over pools of these sparse Boolean (cell=1, non=0) spatial arrays at each time, and then dividing by the horizontal spatial sum, creates horizontal probability arrays $p_{\text{cell}}(x,y)$ which sum to unity. Here x and y are latitude and longitude distances from a central point, with pixel size of about 8km at these low latitudes. The scientific meaning of such p_{cell} maps depends on sensibly constructing relevant data pools, with arrays being rolled or shifted to place a reference cell at the center. Zero padding around the edges contributes to artificial decay of p_{cell} with distance in cell-centered composites, by diluting the probability map for cells near the edges of the $20 \times 20^\circ$ lat-lon box, but no false adjacency signals are introduced. Larger boxes would reduce this edge effect, but would incur more geographical heterogeneities, so the size of quasi-uniform lowland tropical South American land set the size here.

To estimate how the *instantaneous* frequency of cell occurrence depends on distance from another cell, I pooled all 235 pairs (one year apart) of active SA days; and separately the 145 pairs of active SP days. In loops over such pools, zero-padded and cyclically rolled arrays with each center translated to the center were summed. Normalizing these sums to make their horizontal sum equal to unity imparted the defining aspect of a horizontal probability distribution, here denoted $p_{\text{cell}}(x,y,h | \text{cell}@0,0,h)$ for each clock hour h . This

procedure assumes that all the pooled days are equivalent samples drawn from a stable well-defined population.

Results for South America (SA) are shown in Fig. 8. Down the diagonal in blue-yellow colors are \log_2 of the (positive-definite) conditional PD, in 1000km x1000km squares centered on a cell. A tiny ring of zero pixels near the origin is an artifact of the Gaussian smoother + local minimum finder; $1e-99$ was added to make the log operation possible. These PDs are far from uniform, which means the pattern has some information entropy H relative to the reference of a uniform PD, given by the Kullback-Lebler (KL) divergence $\sum_i p_i \log(p_i/q_i)$ with p the actual and q the reference PD.

Besides the near-circular local enhancement on a scale of about 100 km, and a faint crosshair from edge effects, there is speckle (which the eye easily smooths over) that should not be included formally in H . The mesoscale result is somewhat over-sampled spatially by 8km pixels (or, that fine grid is under-sampled in terms of the required amount of data). In the lower-right panel of Fig. 8, $H = 30.6$ *millibits*, out of a possible $S_{\max} = 16.3$ *bits* for a uniform PD over $286 \times 286 = 2^{16.3}$ bins. Block-summing groups of 11×11 pixels retains the central mesoscale peak structure, while eliminating the sampling artifacts and speckle, so it gives a slightly smaller $H = 28.9$ *millibits* out of a much smaller $S_{\max} = 9.4$ *bits* for a uniform PD over $26 \times 26 = 2^{9.4}$ bins. Cylindrical binning even better averages out the speckle, without distorting the fine structure near the origin, but sacrifices the mild anisotropy. The resulting azimuth-summed PD $p_{\text{cell}}(r)$ (which sums to 1 over 49 radius bins r) has 516 *millibits* of H out of 5.61 *bits* for 49 radius bins. An estimate of the improbability of these H values is 2^{-HN} (interpreting KL divergence as in Shlens 2014), where sample size N is at least as great as the largest number of bins in a histogram that well resolves the distributional difference without introducing sampling noise.

Improbability is the “p-value” of a result being a fiction of sampling noise alone. Conservatively, from coarse 11×11 pixel averages, the p-value along the diagonals is stronger than $2^{-(28.9 \text{ millibits} \times 26 \times 26)}$ (about 1 in 500,000) and stronger than $2^{-(516 \text{ millibits} \times 49)}$ (about 1 in 40 million) of the radius-coordinate result, but perhaps not as strong as the speckled result $2^{-(30.6 \text{ millibits} \times 286 \times 286)}$. Perhaps the number of cells, not bins, should be used as in section 3a. The general principle is that degrees of freedom (bins or samples) which contribute little to the signal must not be used to fluff its significance or p-value. In this case, some of the

improbability may indicate structured forcing, and cannot be simply interpreted as a revealed fitness in the past action of an evolutionary process, so further quantification is not helpful.

One notable distinction along the diagonal of Fig. 8 is that at 14UTC (10am local) the central-region probability enhancement is greater (brightest yellows are in upper-left panel). This reflects the fact that deep convection at 10am mainly occurs when a previously developed mesoscale storm is active, a somewhat rare occurrence (and thus a strong enhancement) at a typically low-cell-probability time of day. This signature will be seen again below over the maritime SP area.

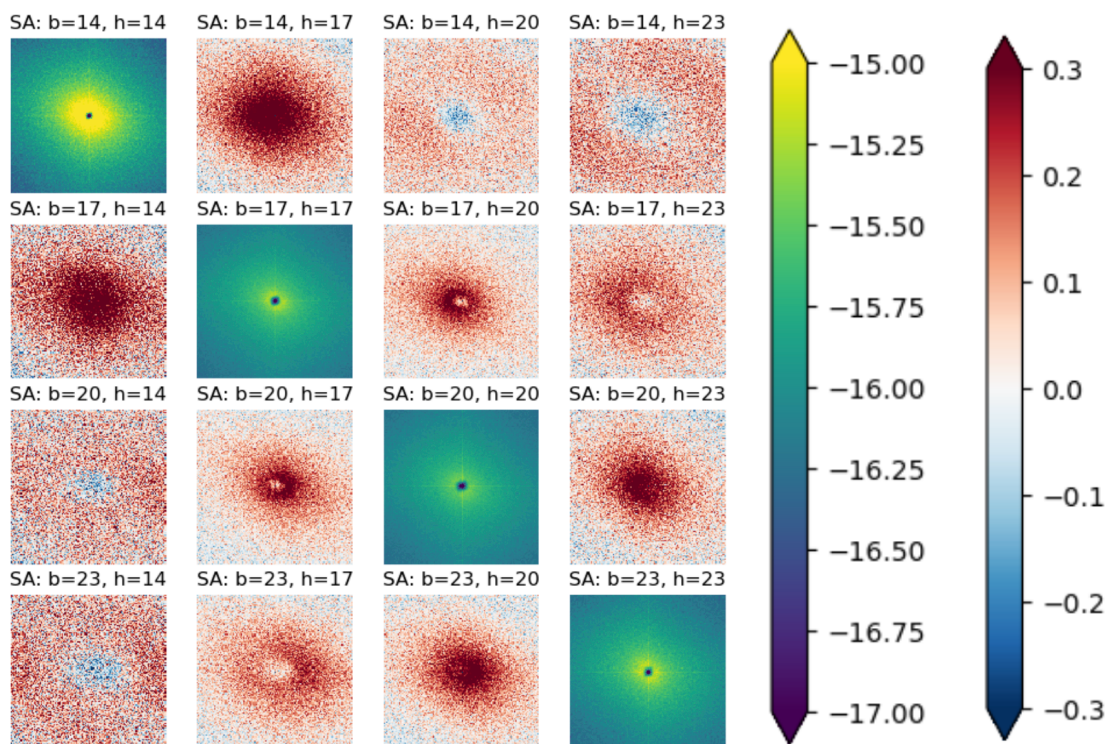


Fig. 8. Frequency composites (probability pattern estimates) through morning-evening hours, for 1000km square areas centered on each cell location in the SA (South America) dataset. On the diagonals (blue-green-yellow scale, positive definite) are instantaneous \log_2 of $p_{\text{cell}}(x,y,h)$ for clock hours h . Off diagonals (blue-red scale) depict differences of \log_2 conditional probability of a cell at an earlier or later clock hour h , given a cell at the center at base hour b one year later or earlier. Base times b and display times h are UTC hours; for LST subtract 4 roughly.

Off the diagonal in Fig. 8 (blue-red color scale) are 1000x1000 km arrays of the log of ratios of conditional probabilities. Specifically, the blue-red colors depict \log_2 of

$$\frac{p_{\text{cell}}(x, y, h \mid \text{cell}@ (0,0, b))}{p_{\text{cell}}(x, y, h \mid \text{cell}@ (0,0, b \text{ 1 year away}))}$$

Here h is the UTC clock hour (column in the figure) and b is a base UTC clock hour (row in the figure). The denominator is constructed from the 235 cell arrays 1 year offset from cell locations at base hour b , for each day in the dataset. This denominator contains the climatological structure, including both geographically anchored features and seasonal effects as transmitted through the 235 selected calendar days in the sample, but lacks the near-origin artifacts of the instantaneous maps along the diagonal panels. No difference was seen between composites based on the MCS days which drove the 235 day sample selection, and the reference days one year later (not shown), so the two offsets (forward & backward by a year) are pooled here to double the sample size. The log of a ratio is a difference of logs, so values can be negative or positive, requiring the blue-red color table.

Again the morning results (left column and upper row) are distinctive, reflecting the influence of uncommon days with cells at 14UTC (10am). On these days, pre-existing mesoscale storms last until about 1pm, and their impact later in the afternoon is a *reduced* probability of new cells (blue central feature in upper-right panel), presumably due to cold pools and/or cloud cover reducing insolation. The lower-left panel is similar in shape to the upper-right, with a blue central feature on about 200 km scale, but it addresses a slightly different question: What *morning* ($b=14\text{UTC}$) cell probability pattern is associated with an evening ($h=23\text{UTC}$) cell at some location? The answer is related to the same phenomenon: mornings which do *not* have mesoscale storms active near that location (blue). Again, these results resemble the oceanic case (discussed below).

The most interesting features of Fig. 8 show the spontaneous succession process through 17-20-23 UTC (roughly 1-4-7 pm local time, columns 3-4 in second row). A cell at the origin at 17 UTC is followed by an expanding ring of enhanced probability (red) at 20 and 23 UTC. This ring reflects new-cell triggering effects from internal waves and gust fronts around cold outflows. However, a blue core indicates cell reductions (stabilization), both by that cold outflow air itself and by surface shading. The difference of information from one time to the next in this upscale growth can be quantified again with KL divergence. For the 20-23 UTC spatial-PD configuration evolution, 7.4 (7.3 when coarse-grained by 11x) *mbits* at 20UTC rises to 8.3 (8.7 when coarse-grained by 11x) *mbits* at 23UTC, as the red ring

expands from ~200km to ~400km around the initial cell while its near-field (~100km) peak value weakens.

A modest east-west anisotropy indicates a mild westward drift velocity, and/or the sun's motion in the sky. It would be interesting to screen inputs by wind or wind shear and see how this anisotropy depends on that. By 23UTC (e.g. b=20, h=23) the blue core has largely disappeared, suggesting that 6-hour-old mesoscale systems lasting past sunset are starting to become generalized cell-enhancers, akin to the mature systems of the morning, and of oceanic SA samples to be examined next.

Figure 9 shows the South Pacific (SP) maritime sample. The diagonal panels show strong mesoscale instantaneous enhancements at all hours, indicative of cell frequency being highly contingent on sizable (several 100s of km) mesoscale convective storms, similar to mornings over SA. This SP region is less active than the SA box, so the cell-conditional enhancements are stronger (brighter colors), and the sample is smaller (145 days) so the patterns are noisier. Red blotches in off-diagonal panels indicate that these storms have typical duration > 6 hours. Across-diagonal symmetry suggests statistically symmetric growth and decay processes, more so than the afternoon patterns over SA in Fig. 8. In this South Pacific Convergence Zone, enhancements often involve trailing fronts from the westerlies to the south, lending a stronger NW-SE orientation to the composite structure. In summary, at all hours, large mesoscale (~500 km) features seem to indicate a 'climax ecology' of such storms governing cell development both day and night, with little indications of the informative initialized-succession process studied over SA after nighttime stabilization.

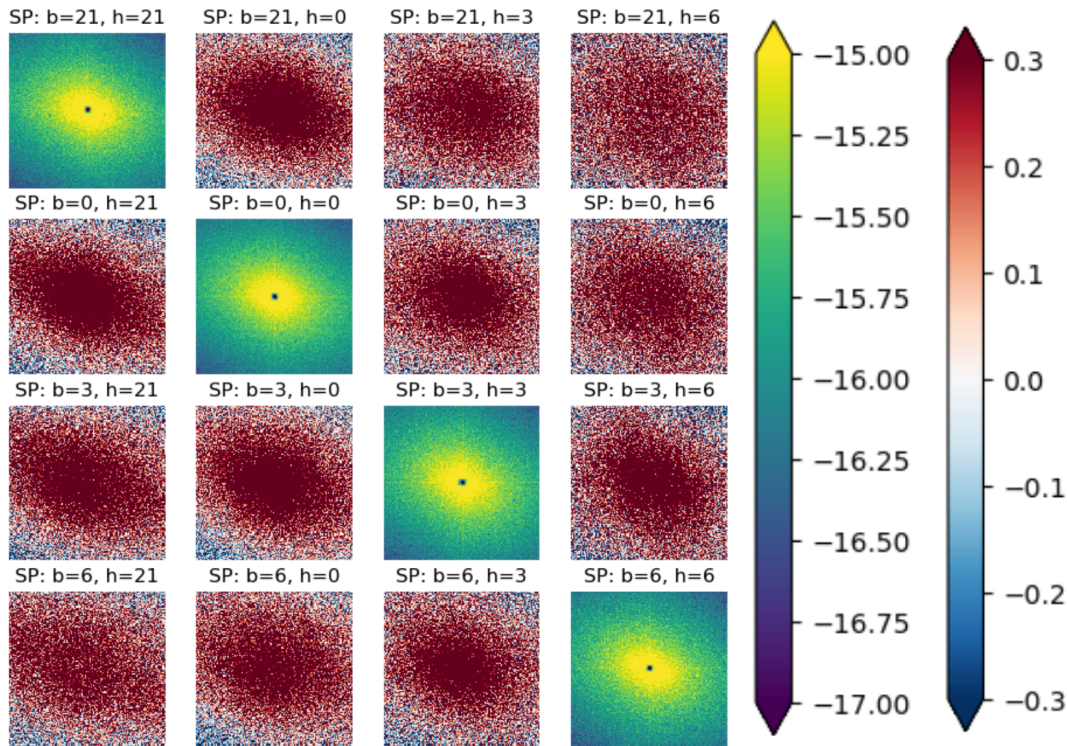


Fig. 9. As in Fig. 8 but for the SP (South Pacific) sample, which is about half as large and thus noisier. Base times b and display times h are UTC hours; for LST add 14 or subtract 10.

5. Summary and discussion

This paper explores the idea that natural selection increases with time the frequency of occurrence of more efficient or ‘fit’ flow configurations that would otherwise be vanishingly improbable. This process is most easily seen after a reset or disturbance of climax or equilibrated conditions, but is salient to the properties of that equilibrium as well. Learning to detect and quantify improbability in cloud patterns, and account for information injected by initial conditions and larger-scale and lower boundary forcing, could reveal the nature of the underlying fitness function. Reconciling or calibrating this inferred or revealed fitness with direct diagnoses of efficiency at convection’s job or telos would illuminate convective organization, and could advance evolutionary theory more broadly. Simulation diagnosis is the most fruitful for such quantitative work.

Preliminary efforts in section 4 illustrated salient analysis tools for shallow and deep cloud fields. Both show that macro (mesoscale) information entropy H , not to be confused with *thermodynamic* entropy at micro (molecular) scales, does grow with time as cloud patterns increase in their degree of horizontal mesoscale pattern development. This

information increase with time obeys the ascendancy principle of Ulanowicz (1997), a macroscopic opposite of the Second Law. Time scales of many hours are indicated, as shallow cloud patterns sprawl to 100s of km especially when precipitation gets involved. For deep convection over South America, the diurnal cycle re-initializes but also clips the succession process. Still, 10s of hours of evolution are implied, as mesoscale configurations which extend for 6-9 hours into evening are still distinctly smaller than the warm-ocean-like patterns seen on mornings when convective systems have survived the night. This comports with general experience with MCS lifetimes (Houze 2018, Chen et al. 2023).

If information-based improbability estimates for horizontal patterns do serve as a proxy for convection's efficiency at its job (lowering the center of gravity of its embedding airmass), then convective-adjustment parameterization ideas may need both rather long timescales, and adaptive or moving targets defining what is a "neutral" profile. Work to establish these bulk parameterizations offers new quantitative uses of high spatial resolution data, with which our field is blessed to embarrassment, or even burdened: For instance, data assimilation systems routinely use crude averaging to "super-ob" excessive samples.

The quantitative improbability implied by H values and differences (K-L divergences) remain something of a puzzle. Can the inferred-fitness portion of the improbability of a configuration distinguish between strength of a single selection and depth of iterative selection? Synthetic data studies using cellular automata as forward models (e.g. Bengtsson et al. 2013, 2022), using the empirical probability patterns of Fig. 8 in an iterated way, could clarify how much about an evolutionary selection process can be inferred from its outputs.

Other researchers study convecting-airmass configuration inertia or "memory" (Colin et al. 2019, Daleu et al. 2020, Hwong et al. 2023), distinct from mean-profile thermal inertia. Small convecting domains reach their (stunted) "climax ecology" much sooner than larger ones (Lamaakel et al. 2023), and an early truncation of evolving configurations can be expected to affect airmasses and their contrasts on larger scales, such as over tropical ocean vs. land where the diurnal cycle truncates evolution. Cloud model-based work can shade directly into experiments with super-parameterized (SP) models as those become more affordable, to illuminate what is at stake when clipping configuration evolution or memory.

Is airmass *age* the best axis for configuration evolution, or should it be rescaled by energy throughput (Fig. 6b), or its square root (eddy turnover time) or something? A statistical model of the evolution of H in the Cloud Botany dataset (Janssen et al 2023) could do much more

than Fig. 6 managed to. How can we account for the “guilds” of distinct but mutually contingent configuration-shapers (shear-induced cloud streets; cloud lines from plane wave resonances like Balaji and Clark 1988, Lane and Zhang 2011, Stephan et al. 2021; precipitation-driven patterns, all in the presence of larger-scale forcings? Can answers be worked toward in atlases of interaction sub-process maps on Lotka-Volterra-like spaces, as in Figs. 3-4. Might that be a common space to reconcile works on convective organization as defined by others as well (e.g. “memory” works, or Masunaga et al. 2021)?

Synoptic-scale flow is also convection: vertical, gravitationally driven, but also latitudinal and constrained by angular momentum. Still, it is philosophically similar in that time acts to naturally select winning configurations or strategies (however indexed; spectral or spatial). These ideas are implicit in traditional fluid instability discourse, and adjustment ideas stand there too -- as an assumption that the most-capable convective process arises instantly and devours all available energy, in the hard adjustment limit. Between these endpoints of physics culture’s parsimony lies an ecology-like space of nonunique, contingent, but ultimately directed (by selection) evolutionary processes. Might impactful statistics, like the frequency of high-impact flow configurations, like stationary waves or blocking, be understood usefully in evolutionary terms? Do fitness-accumulating structures or configurations win a competition against easy and short-lived but inefficient random eddies? This ‘survival of the fittest’ postulate skates close to tautology, if fitness is defined as whatever survives. But evolutionary logic usefully unlocks new insights and questions, and the phenomenon of convection admits physical descriptions with enough rigor to avoid the pitfall.

Darwinian evolution ideas helped biology turn its corner from taxonomy to systematics, greatly aided by modern genetics as a final arbiter -- a role that simulation can play in convection. Principles like ascendancy (Ulanowicz 1997) are not a prediction technology, indeed are little more than an arrow of time, opposite the Second Law of thermodynamics. The enterprise of cloud pattern description might be usefully oriented by this same simple magnetizing concept, with the concept of inferred fitness as both our way of detecting and measuring evolution, and a driving reason to care about how it plays out. Perhaps convection can be fruitfully viewed as a simple version of life, not only as a complicated phenomenon of statistical and mechanical physics.

Acknowledgments.

This material is based upon work supported by the National Science Foundation under Grant numbers 2141492 and 2318221, and NASA grant NASA grant NNX09AD22G. The Cloud Botany project is appreciated for excellent data resource and access codes, along with NOAA Gridsat team for that excellent online resource.

Data Availability Statement.

All codes and documentation are in Jupyter notebooks at the open repository: <https://github.com/brianmapes/EvolutionaryConvection>. All data used are available publicly online, except the MCS dataset, courtesy of Dr. Xingchao Chen (Chen et al. 2023), used only lightly to sample some days in the rainy season (those exact days are listed in the download code notebook).

REFERENCES

- Aaronson, S., S. M. Carroll, and L. Ouellette, 2014: Quantifying the Rise and Fall of Complexity in Closed Systems: The Coffee Automaton. <https://doi.org/10.48550/arXiv.1405.6903>
- Adames, Á. F., S. W. Powell, F. Ahmed, V. C. Mayta, and J. D. Neelin, 2021: Tropical Precipitation Evolution in a Buoyancy-Budget Framework. *J. Atmos. Sci.*, **78**, 509–528, <https://doi.org/10.1175/JAS-D-20-0074.1>.
- Albrecht, B., and Coauthors, 2019: Cloud System Evolution in the Trades (CSET): Following the Evolution of Boundary Layer Cloud Systems with the NSF–NCAR GV. *Bull. Amer. Meteor. Soc.*, **100**, 93–121, <https://doi.org/10.1175/BAMS-D-17-0180.1>.
- Arakawa, A., 2004: The cumulus parameterization problem: Past, present, and future. *J. Climate*, **17**, 2493–2525.
- Arakawa, A., and W. H. Schubert, 1974: Interaction of a cumulus cloud ensemble with the large- scale environment, Part I. *J. Atmos. Sci.*, **31**, 674–701.
- Balaji, V., and T. L. Clark, 1988: Scale Selection in Locally Forced Convective Fields and the Initiation of Deep Cumulus. *J. Atmos. Sci.*, **45**, 3188–3211, [https://doi.org/10.1175/1520-0469\(1988\)045<3188:SSILFC>2.0.CO;2](https://doi.org/10.1175/1520-0469(1988)045<3188:SSILFC>2.0.CO;2).

Bartlett, Stuart, and Michael L. Wong. 2020. "Defining Lyfe in the Universe: From Three Privileged Functions to Four Pillars" *Life* 10, no. 4: 42. <https://doi.org/10.3390/life10040042>

Ben-Naim, Arieh, 2008: *A Farewell to Entropy: Statistical Thermodynamics Based on Information*. World Scientific, 410pp. ISBN 978-981-270-706-2

Bengtsson, L., Steinheimer, M., Bechtold, P., & Geleyn, J.-F. (2013). A stochastic parameterization for deep convection using cellular automata. *Quarterly Journal of the Royal Meteorological Society*, 139, 1533–1543. <https://doi.org/10.1002/qj.2108>

Bengtsson, L., L. Gerard, J. Han, M. Gehne, W. Li, and J. Dias, 2022: A Prognostic-Stochastic and Scale-Adaptive Cumulus Convection Closure for Improved Tropical Variability and Convective Gray-Zone Representation in NOAA's Unified Forecast System (UFS). *Mon. Wea. Rev.*, **150**, 3211–3227, <https://doi.org/10.1175/MWR-D-22-0114.1>.

Brune, S, Buschow, S, Friederichs, P., 2021: The local wavelet-based organization index – Quantification, localization and classification of convective organization from radar and satellite data. *QJR Meteorol Soc.* 2021; 1853–1872. <https://doi.org/10.1002/qj.3998>

Cantrell, S., C. Cosner and S. Ruan, Eds, 2010: *Spatial Ecology*. Chapman & Hall/CRC Mathematical Biology Series, 360 pp. ISBN 9781420059854

Carroll, S., 2016: *The Big Picture: On the Origins of Life, Meaning, and the Universe Itself*. Dutton, 480 pp. ISBN 978-0-525-95482-8.

Chen, X., Leung, L. R., Feng, Z., & Yang, Q. (2023). Environmental controls on MCS lifetime rainfall over tropical oceans. *Geophysical Research Letters*, 50, e2023GL103267. <https://doi.org/10.1029/2023GL103267>

Colin, M., S. Sherwood, O. Geoffroy, S. Bony, and D. Fuchs, 2019: Identifying the Sources of Convective Memory in Cloud-Resolving Simulations. *J. Atmos. Sci.*, **76**, 947–962, <https://doi.org/10.1175/JAS-D-18-0036.1>.

Daleu, C. L., Plant, R. S., Woolnough, S. J., Stirling, A. J., & Harvey, N. J. (2020). Memory properties in cloud-resolving simulations of the diurnal cycle of deep convection. *Journal of Advances in Modeling Earth Systems*, 12, e2019MS001897. <https://doi.org/10.1029/2019MS001897>

Dawkins, R., 1976: *The Selfish Gene*. Oxford University Press, 352 pp. ISBN: 9780192177735

Denby, L., 2020: Discovering the Importance of Mesoscale Cloud Organization Through Unsupervised Classification. *Geophysical Research Letters*, 47 (1).
<https://onlinelibrary.wiley.com/doi/10.1029/2019GL085190>

Denby, L., 2023: Charting the Realms of Mesoscale Cloud Organisation using Unsupervised Learning. <https://arxiv.org/pdf/2309.08567.pdf>

Dennett, D.C., 1996: *Darwin's Dangerous Idea: Evolution and the Meanings of Life* (Simon & Schuster, 586pp. [ISBN 0-684-82471-X](https://www.amazon.com/dp/068482471X))

Dennett, D.C., 2017: *From Bacteria to Bach and Back. The Evolution of Minds*. Penguin Press, 496pp. ISBN 978-0-393-24207-2.

Emanuel, K. A., 1991: The theory of hurricanes, *Ann. Rev. Fluid Mech.* 23, 179–196.

Fleming, J., 2007: A 1954 color painting of weather systems as viewed from a future satellite. *Bull. Amer. Meteor. Soc.*, 88, 1525-1527.

Freitas, S. R., Grell, G. A., Chovert, A. D., Silva Dias, M. A. F., & de Lima Nascimento, E. (2024). A parameterization for cloud organization and propagation by evaporation-driven cold pool edges. *Journal of Advances in Modeling Earth Systems*, 16, e2023MS003982. <https://doi.org/10.1029/2023MS003982>

Golan, A., and Harte, J., 2022: Information theory: A foundation for complexity science. *Proc Natl Acad Sci.* 119(33):e2119089119. doi: 10.1073/pnas.2119089119.

Gregory, T.R. Understanding Natural Selection: Essential Concepts and Common Misconceptions. *Evo Edu Outreach* 2, 156–175 (2009). <https://doi.org/10.1007/s12052-009-0128-1>

Haerter, J. O. (2019). Convective self-aggregation as a cold pool-driven critical phenomenon. *Geophysical Research Letters*, 46, 4017–4028.
<https://doi.org/10.1029/2018GL081817>

Hohenegger, C., and B. Stevens, 2013: Preconditioning Deep Convection with Cumulus Congestus. *J. Atmos. Sci.*, 70, 448–464, <https://doi.org/10.1175/JAS-D-12-089.1>.

Houze, R. A., Jr., 2018: 100 years of research on mesoscale convective systems. *AMS Meteor. Monogr.*, 59, 17.1-17.54.

Hwong, Y.-L., M. Colin, P. Aglas-Leitner, C.J. Muller, S.C. Sherwood, 2023: Assessing Memory in Convection Schemes Using Idealized Tests. JAMES, submitted. Available at <https://essopenarchive.org/doi/full/10.22541/essoar.168056812.21996560>

Janssens, M. , Vilà-Guerau de Arellano, J. , Scheffer, M. , Antonissen, C. , Siebesma, A. P. , & Glassmeier, F. (2021). Cloud patterns in the trades have four interpretable dimensions. *Geophysical Research Letters*, 48, e2020GL091001. <https://doi.org/10.1029/2020GL091001>

Jansson, F., and Coauthors. 2023: Cloud Botany: Shallow cumulus clouds in an ensemble of idealized large-domain large-eddy simulations of the trades. 10.22541/essoar.168319841.11427814/v1.

Khouider, B., 2019: *Models for Tropical Climate Dynamics: Waves, Clouds, and Precipitation*, Springer, 303pp, ISBN : 978-3-030-17774-4. <https://doi.org/10.1007/978-3-030-17775-1>

Knapp, K. R., S. Ansari, C. L. Bain, M. A. Bourassa, M. J. Dickinson, C. Funk, C. N. Helms, C. C. Hennon, C. D. Holmes, G. J. Huffman, J. P. Kossin, H.-T. Lee, A. Loew, and G. Magnusdottir, 2011: Globally gridded satellite (GridSat) observations for climate studies. *Bulletin of the American Meteorological Society*, 92, 893-907. [doi:10.1175/2011BAMS3039.1](https://doi.org/10.1175/2011BAMS3039.1)

Lamaakel, O.; R. Venters; J. Teixeira; G. Matheou, 2023: Computational Domain Size Effects on Large-Eddy Simulations of Precipitating Shallow Cumulus Convection. *Atmosphere*, 14, 1186. <https://doi.org/10.3390/atmos14071186>

Lane, T. P., and F. Zhang, 2011: Coupling between Gravity Waves and Tropical Convection at Mesoscales. *J. Atmos. Sci.*, **68**, 2582–2598, <https://doi.org/10.1175/2011JAS3577.1>.

Mapes, B. E., S. Tulich, T. Nasuno, and M. Satoh, 2008: Predictability aspects of global aqua-planet simulations with explicit convection. *J. Meteor. Soc. Japan*, 86A, 175-185.

Mapes, B., Chandra, A.S., Kuang, Z. and P. Zuidema. Importance Profiles for Water Vapor. *Surv Geophys* 38, 1355–1369 (2017). <https://doi.org/10.1007/s10712-017-9427-1>, free at <https://rdcu.be/dwPyM>

Mapes, B., & Neale, R. (2011). Parameterizing convective organization to escape the entrainment dilemma. *Journal of Advances in Modeling Earth Systems*, 3, M06004, doi:10.1029/2011MS000042.

Mapes, B. E., 2021: Toward form-function relationships for mesoscale structure in convection. *J. Meteor. Soc. Japan*, 99, 847–878, <https://doi.org/10.2151/jmsj.2021-041>.

Masunaga, H., C. E. Holloway, H. Kanamori, S. Bony, and T. H. M. Stein, 2021: Transient Aggregation of Convection: Observed Behavior and Underlying Processes. *J. Climate*, **34**, 1685–1700, <https://doi.org/10.1175/JCLI-D-19-0933.1>.

Morrison, H., J. M. Peters, A. C. Varble, S. Giangrande, W. M. Hannah, 2019: Thermal chains and entrainment in cumulus updrafts, Part 1: Theoretical description. *J. Atmos. Sci.*, 77, 3637-3660. doi:10.1175/JAS-D-19-0243.1

Muller CJ, Yang D, Craig G, Cronin T, Fildier B, Haerter JO, Hohenegger C, Mapes B, Randall D, Shamekh S, Sherwood SC. 2022. Spontaneous aggregation of convective storms. *Annual Review of Fluid Mechanics*. 54, 133–157.

Newton, Jonathan. 2018: Evolutionary Game Theory: A Renaissance. *Games* 9, no. 2: 31. <https://doi.org/10.3390/g9020031>

Nicolis, G. & Prigogine, I., 1977: *Self-Organization in Nonequilibrium Systems: From Dissipative Structures to Order through Fluctuations*. Wiley, New York, 512pp. ISBN-13: 978-0471024019.

Nober, F. J., and H-F. Graf, 2005: A new convective cloud field model based on principles of self-organisation. *Atmos. Chem. Phys.*, **5**, 2749–2759.

Palmer, T., 2022: *The Primacy of Doubt: From Quantum Physics to Climate Change, How the Science of Uncertainty Can Help Us Understand Our Chaotic World*. Basic Books, 320 pp. ISBN-13 : 978-1541619715

Parrondo, J., Horowitz, J. & Sagawa, T. Thermodynamics of information. *Nature Phys* **11**, 131–139 (2015). <https://doi.org/10.1038/nphys3230>

Pauluis, O. and I. M. Held, 2002: Entropy budget of an atmosphere in radiative-convective equilibrium. Part II: Latent heat transport and moist processes, *J. Atmos. Sci.* 59, 140–149.

Pritchard, M. S., C. S. Bretherton, and C. A. DeMott, 2014: Restricting 32–128 km horizontal scales hardly affects the MJO in the Superparameterized Community Atmosphere Model v.3.0 but the number of cloud-resolving grid columns constrains vertical mixing. *J. Adv. Model. Earth Syst.*, 6, 723–739.

Rajković, M., M. Milovanović, M. M. Škorić, 2017: Quantifying self-organization in fusion plasmas. *Phys. Plasmas* 1 May 2017; 24 (5): 052303. <https://doi.org/10.1063/1.4982612>

Ramirez, J. A., R. L. Bras, 1990: Clustered or regular cumulus cloud fields: The statistical character of observed and simulated cloud fields, *J. Geophys. Res.*, 95, 2035–2045.

Randall, D.A. and G.J. Huffman, 1980: A Stochastic Model of Cumulus Clumping. *J. Atmos. Sci.*, 37, 2068–2078, [https://doi.org/10.1175/1520-0469\(1980\)037<2068:ASMOCC>2.0.CO;2](https://doi.org/10.1175/1520-0469(1980)037<2068:ASMOCC>2.0.CO;2)

Rasp, S., Schulz, H., Bony, S. and Stevens, B., 2020. Combining crowd-sourcing and deep learning to explore the meso-scale organization of shallow convection. *Bulletin of the American Meteorological Society*. <https://doi.org/10.1175/BAMS-D-19-0324.1>

Romps, D. M., 2008: The dry-entropy budget of a moist atmosphere. *J. Atmos. Sci.* 65, 3779–3799.

Rosas, F.; Mediano, P.A.M.; Ugarte, M.; Jensen, H.J, 2018: An Information-Theoretic Approach to Self-Organisation: Emergence of Complex Interdependencies in Coupled Dynamical Systems. *Entropy*, 20, 793. <https://doi.org/10.3390/e20100793>

Sakaeda, N., & Torri, G. (2022). The behaviors of intraseasonal cloud organization during DYNAMO/AMIE. *Journal of Geophysical Research: Atmospheres*, 127, e2021JD035749. <https://doi.org/10.1029/2021JD035749>

Schrödinger, E., 1944: *What Is Life?* Cambridge University Press, 194 pp. ISBN 0-521-42708-8

Schulz, H., Eastman, R., & Stevens, B. (2021). Characterization and evolution of organized shallow convection in the downstream North Atlantic trades. *Journal of Geophysical Research: Atmospheres*, 126, e2021JD034575. <https://doi.org/10.1029/2021JD034575>

Schulz, H., & Stevens, B. (2023). Evaluating large-domain, hecto-meter, large-eddy simulations of trade-wind clouds using EUREC4 A data. *Journal of Advances in Modeling Earth Systems*, 15, e2023MS003648. <https://doi.org/10.1029/2023MS003648>

Shalizi, C.R.; Shalizi, K.L.; Haslinger, R. Quantifying self-organization with optimal predictors. *Phys. Rev. L* **2004**, 93, 118701.

Shamekh S, Lamb KD, Huang Y, Gentine P, 2023: Implicit learning of convective organization explains precipitation stochasticity. *Proc Natl Acad Sci*. 16;120(20):e2216158120. doi: 10.1073/pnas.2216158120.

Sharma, A., Czégel, D., Lachmann, M. *et al.*, 2023: Assembly theory explains and quantifies selection and evolution. *Nature* **622**, 321–328. <https://doi.org/10.1038/s41586-023-06600-9>

Shlens, J., 2014: Notes on Kullback-Leibler Divergence and Likelihood. <https://arxiv.org/abs/1404.2000>.

Singh, M.S., and M.E. O'Neill, 2022: The climate system and the second law of thermodynamics. *Rev. Mod. Phys.*, 94, <https://link.aps.org/doi/10.1103/RevModPhys.94.015001>.

Stein, T. H. M., C. E. Holloway, I. Tobin, and S. Bony, 2017: Observed Relationships between Cloud Vertical Structure and Convective Aggregation over Tropical Ocean. *J. Climate*, **30**, 2187–2207, <https://doi.org/10.1175/JCLI-D-16-0125.1>.

Stephan, C.C., Žagar, N. & Shepherd, T.G., 2021: Waves and coherent flows in the tropical atmosphere: New opportunities, old challenges. *Q J R Meteorol Soc*, 147: 2597–2624. Available from: <https://doi.org/10.1002/qj.4109>

Stevens, B., M. Satoh, L. Auger, J. Biercamp, C. S. Bretherton, X. Chen, P. Düben, F. Judt, M. Khairoutdinov, D. Klocke, C. Kodama, L. Kornbluh, S.-J. Lin, P. Neumann, W. M. Putman, N. Röber, R. Shibuya, B. Vanniere, P. L. Vidale, N. Wedi, and L. Zhou, 2019: DYAMOND: The DYnamics of the Atmospheric general circulation Modeled On Non-hydrostatic Domains. *Prog. Earth Planet. Sci.*, 6, 61, doi:10.1186/s40645-019-0304-z.

Sullivan, S. C., Schiro, K. A., Stubenrauch, C., & Gentine, P. (2019). The response of tropical organized convection to El Niño warming. *Journal of Geophysical Research: Atmospheres*, 124, 8481–8500. <https://doi.org/10.1029/2019JD031026>

Tsai, W.-M., and B. E. Mapes, 2022: Evidence of Aggregation Dependence of 5°-Scale Tropical Convective Evolution Using a Gross Moist Stability Framework. *J. Atmos. Sci.*, **79**, 1385–1404, <https://doi.org/10.1175/JAS-D-21-0253.1>.

Tsai, W.-M., 2023: *Exploring Vapor-Convection Interactions and Convective Organization over Multiple Scales*. PhD dissertation, <https://scholarship.miami.edu/esploro/outputs/doctoral/Exploring-Vapor-Convection-Interactions-and-Convective-Organization/991031765817602976#file-0>

Tulich, S. N. (2015). A strategy for representing the effects of convective momentum transport in multiscale models: Evaluation using a new superparameterized version of the Weather Research and Forecast model (SP-WRF). *Journal of Advances in Modeling Earth Systems*, **7**, 938–962. <https://doi.org/10.1002/2014MS000417>

Ulanowicz, R.E., 1997: *Ecology, The Ascendant Perspective*. Columbia University Press, 201 pp. ISBN:9780231108294.

Ulanowicz, R.E., 2009: *A Third Window: Natural Life Beyond Newton and Darwin*. Templeton Press, 196 pp. ISBN:9781599471549

Vieweg, P.P., J. D. Scheel, and J. Schumacher, 2021: Supergranule aggregation for constant heat flux-driven turbulent convection, *Phys. Rev. Res.* **3**, 013231

Vieweg, P.P., 2023: Supergranule aggregation: a Prandtl number-independent feature of constant heat flux-driven convection flows. Submitted to *J. Fluid Mech.*; available at <https://arxiv.org/pdf/2311.08327.pdf>

Wing, A. A., Emanuel, K. A., Holloway, C. E., & Muller, C. (2017). Convective self-aggregation in numerical simulations: A review. *Surveys in Geophysics*, **38**(6), 1173–1197.

Wong, M.L., C. E. Cleland, D. Arend, S. Bartlett, H. J. Cleaves, H. Demarest, A. Prabhu, J. I. Lunine, & R. M. Hazen (2023). On the roles of function and selection in evolving systems. *Proceedings of the National Academy of Sciences*, **120**(43), e2310223120.

Xu, K.-M., Hu, Y., & Wong, T. (2019). Convective aggregation and indices examined from CERES cloud object data. *Journal of Geophysical Research: Atmospheres*, **2019**, 124: 13604–13624. <https://doi.org/10.1029/2019JD030816>

Xu, K.-M., Zhou, Y., Sun, M., Kato, S., & Hu, Y. (2023). Observed Cloud Type-Sorted Cloud Property and Radiative Flux Changes with the Degree of Convective Aggregation

from CERES Data. *Journal of Geophysical Research: Atmospheres*, 128, e2023JD039152.
<https://doi.org/10.1029/2023JD039152>

Yano, J.-I., and R. S. Plant, 2016: Generalized convective quasi-equilibrium principle. *Dyn. Atmos. Oceans*, **73**, 10–33, <https://doi.org/10.1016/j.dynatmoce.2015.11.001>.

Zipser, E. J., 1970: The Line Islands Experiment, its place in tropical meteorology and the rise of the fourth school of thought. *Bull. Amer. Meteor. Soc.*, 51, 1136-1147.

Zuidema, P., and Coauthors, 2012: On Trade Wind Cumulus Cold Pools. *J. Atmos. Sci.*, 69, 258–280, <https://doi.org/10.1175/JAS-D-11-0143.1>.